

CORTICAL BLOOD FLOW IMAGING WITH A PORTABLE MEMS BASED 2-PHOTON FLUORESCENCE MICROENDOSCOPE

W. Piyawattanametha¹⁻³, O. Solgaard², and M. J. Schnitzer¹

¹NECTEC, Pathumthani, Thailand 12120, ²Edward L. Ginzton Laboratory, Stanford University Stanford, CA 94305³, James H. Clark Center for Biomedical Engineering & Sciences, Stanford University Stanford, CA 94305

ABSTRACT

We present a portable microendoscope based on a microelectromechanical systems (MEMS) scanner, compound gradient refractive index micro-lenses and a photonics bandgap fiber (PBF). It overcomes the size ($2.0 \times 1.9 \times 1.1 \text{ cm}^3$) and weight (less than 3 grams) limitations of conventional two-photon fluorescence microscopy toward freely moving subjects. The microendoscope utilizes a PBF for laser excitation and large core fiber for fluorescence collection. We demonstrated cortical blood flow imaging in live mice with transverse (Δx) and axial resolutions (Δz) of $1.6 \mu\text{m}$ and $13.5 \mu\text{m}$, respectively.

KEYWORDS

neuroscience, scanner, 2-photon, MEMS, fluorescence

INTRODUCTION

The relationship of neural network activity and the blood flow is the basis for brain homeostasis which is described as the balanced of blood flow in nutrient delivery and removal of excess heat and metabolites. In recent years, many research groups have extensively investigated these connections through individual capillaries in both the pia matter level and the cortex to the state of normal and the diseased brain [1, 2] in order to gain in-depth fundamental knowledge of homeostasis. Two-photon fluorescence microscopy (2PFM) has been identified as an important imaging technique that enables visualization of blood flow in deep cortical microvasculature due to its unique ability to perform high resolution imaging very deep inside highly scattering tissues with reduced both photobleaching and phototoxicity [3, 4]. To date, 2PFM technique for *in vivo* blood flow study has only been demonstrated in anesthetized subjects with a bulky benchtop instrument setup. However, correlation of blood flow characteristics with behavior is not possible during anesthesia. Two main methods to further utilize 2PFM in freely moving subjects are head-fixed to the microscope [5] and portable head-mounted microendoscope [6]. The first technique provides high quality images but has limited behavioral experiments that can be performed on. The second technique can potentially expand behavioral studies with slight degradation in imaging performance. As a result, there is lots of interest in the development of

portable 2PFMs that enables deep brain functional imaging in freely moving subjects [6, 7]. Several key parameters to enable miniaturization of the 2PFM systems are rapid beam scanning and data acquisition, high efficiency in both light excitation and collection, and compact beam scanning mechanism with small scanning element footprint size. With all the technological advancement so far, the latter development is still a major obstacle in 2PFM miniaturization. Scanning mechanisms that use either a double-clad fiber (DCF) [8, 9] or a hollow-core PBF [7, 10] combined with piezoelectric or shape memory alloy actuators are deployed due to their relatively simple constructions and potentially achieving small probes diameter. However, this scanning technique has limited abilities in random-access or selective scanning pattern [11] with high acquisition frame rate due to choice of the actuators used. Most importantly, batch fabrication for mass production to aid low cost imaging applications is not possible which can limit a ubiquitous use of these probes in clinical applications. Recently, several research groups have chosen to use two-dimensional (2-D) MEMS scanners to provide elegant solutions in 2PFM miniaturization [11-15]. High speed scanning translating to a very high acquisition frame rate can be realized through relative high young's modulus of silicon micromachined torsion beams of the MEMS scanner [16]. Moreover, large mirror area and angular rotation with a compact foot print from the MEMS scanner design will help increase the number resolvable spots and enable a miniature two-photon fluorescence microendoscope (2PFME) [11].

METHOD

A. SCANNING MECHANISM

Generally, there are two main methods of imaging forming with MEMS scanners—Lissajous and raster scans. Lissajous scan is driven by exciting both axes of a MEMS scanner at its resonant frequency. This method tends to over-sample and under-sample the data at the image periphery and center (non-uniform sampling), respectively. Therefore, typical images from this method are required to have long averaging time [14] and in some heavy cases post-image processing [15] in order to obtain high quality images as images from a desktop system. On the other hand, raster scanning [11-13] is driven by running only one axis at resonant while

the other is running in a DC operating mode. With this scan method, uniform sampling can be achieved across the sample resulting in high quality images with less averaging time.

Even though the reported miniature 2PFM systems in [15] (0.46 NA, $\Delta x = 1.64 \mu\text{m}$) and (0.9 NA, $\Delta x = 1.35 \mu\text{m}$) achieve good transverse resolutions, their form factors are still too large (centimeter-scale) for their intended applications. While in [13], the miniaturized probe seems to have a good form factor but lacking the resolution from the choice of low NA optics (0.17 effective NA) in the probe. All in all, none of the above MEMS based 2PFMEs is able to demonstrate imaging in live animal subjects. We report here a portable 2PFME consists of a 2-D MEMS scanner, a gradient refractive index (GRIN) lens assembly, and a flexible hollow-core PBF capable of imaging in live subjects. The ultimate goal of the project is toward the imaging in freely moving subjects. Figure 1(a) provides a photograph of the MEMS based 2PFME unit with one packaging side off. Internal components show GRIN lens assembly mounted inside the imaging head unit and electrical control wires for a micromotor and a MEMS scanner. The total weight of the unit is less than 3 g. The MEMS scanner mounted on a double-sided printed circuit board (PCB) [Figure 1(b)] has a gimbal structure that facilitates rotation in two dimensions with minimal mechanical crosstalk between axes and is actuated by self-aligned electrostatic vertical comb actuators to provide greater actuation force than parallel plate counterparts. The scanners are batch fabricated on a double silicon-on insulator (SOI) wafer with 4 deep reactive ion-etching (DRIE) steps to realize the scanners [16]. The MEMS scanner die size is $3.2 \times 3.0 \text{ mm}^2$. The PCB ($5 \times 6 \text{ mm}^2$) is fabricated with a plated-through-hole technology to route electrical connections from MEMS scanner chip on the front side to the electrical control wires on the back side.

B. IMAGING HEAD

Figure 1(c) provides a schematic of the 2FME. The unit consists of a focusing shuttle, a coupling lens mount, an imaging head unit, a GRIN lens assembly, a baseplate, and a protective housing. Both protective housing and imaging head unit are fabricated from a conductive plastic—carbon-filled polyetheretherketone (PEEK) to minimize any floating charges in the material that could affect the performance of the MEMS scanner during operation. To deliver excitation light we coupled

pulses (100-150 fs, center wavelength 790-810 nm) from a Ti:sapphire laser into the lowest-order of the hollow-core PBF for efficient pulse delivery with minimal distortion [red arrow in Fig. 1(d)]. The laser beam is first collimated by using an aspherical lens [LightPath Technologies, Inc. 350140] before it reflects off the MEMS mirror surface. The collimated beam enters the GRIN lens assembly (GRINTEC, GmbH) consisting of a GRIN lens beam expander set, a microprism and an endoscopic objective lens in order to first expand the beam and then focus the beam down to a very small spot size. The beam expander is one 2-mm-diameter GRIN relay lens (0.2 NA, 0.27 pitch) and 1.8-mm diameter GRIN relay lens (0.2 NA, 0.22 pitch). The microprism cube serving as a dichroic mirror has volume of $2 \times 2 \times 2 \text{ mm}^3$. The endoscopic objective lens is a 1-mm diameter lens (0.2 NA, 0.23 pitch). The GRIN lens assembly NAs for beam excitation and collection paths are 0.51 and 0.62, respectively. A multimode polymer fiber (2-mm-diameter core) positioned above the microprism captures fluorescence photons [green arrow in Fig. 1(d)] returning through the GRIN lens assembly.

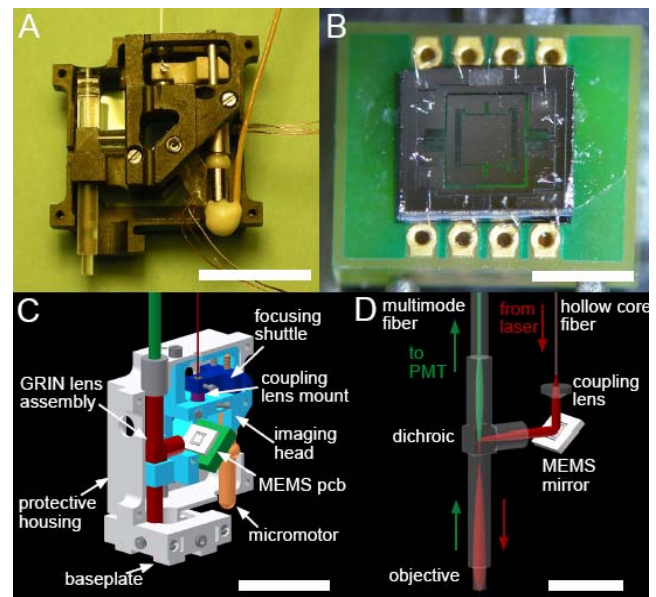


Fig. 1: a, Photograph of the portable 2PFME. Electrical control wires in the photograph are for MEMS scanner and micromotor b, photograph of a MEMS scanner die ($3.2 \times 3.0 \text{ mm}^2$) wire-bonded onto the PCB ($5 \times 6 \text{ mm}^2$) electrodes. c, Computer-aided-design (CAD) model of portable 2PFME mounted on the base plate and with one side open to show internal components. d, CAD model display excitation and collection beam paths inside the portable 2PFME. Red, excitation laser beam; Green, collection fluorescence signal. The scale bars are 1 cm.

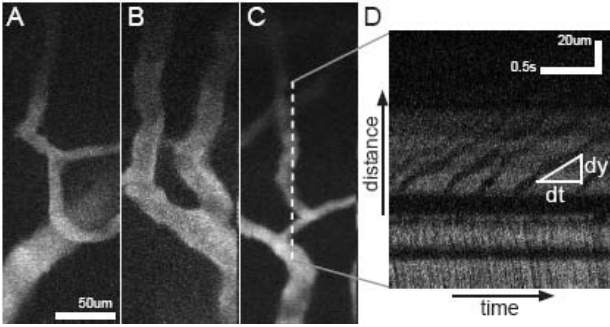


Fig. 3: a to c, En face fluorescence images of various neocortical capillaries acquired at 4 Hz with averaging time of 2 s. d to f, Linescan images of the motion of RBCs in capillaries. The linescan images are obtained by turning off the actuation voltages to the slow- or DC-axis while keep the resonant-axis running at the mechanical resonant frequency (560 Hz) of the MEMS scanner. The velocities of the RBCs in each linescan image were calculated by comparing the change in time (Δt) and the change in distance (Δy) that each streak in the image spans. For each streak, $\Delta y/\Delta t$ was found by marking the region bounded by the streak and then measuring the slope of the midline of this region.

The MEMS scanner has 5 control wires-- a ground and four voltage signal lines, two lines for each axis (x and y- axes). A raster scan pattern (y-axis operating in resonant mode and x-axis operating in DC mode) is used to obtain images with the MEMS scanner. Because the force provided by each comb bank grows linearly with the square of the applied voltage, we drive each opposing comb bank pair with actuating driving signals that are 180° out of phase. This help increase the linear range of the angular scan as a function of drive voltage due to cancellation of the leading quadratic voltage terms. In DC operation, the maximum optical angular ranges for the inner and outer axes are about $\pm 5^\circ$ at 60 V_{dc} and $\pm 4.3^\circ$ at 180 V_{dc}, respectively [Figure 2(a)]. In AC operation, the scan rate for each axis can be adjusted from near dc to over the mechanically resonant frequencies of 1.08 kHz and 0.56 kHz for the inner and the outer gimbal, respectively [Figure 2(b)].

RESULTS & CONCLUSIONS

In our experiment, the maximum FOV is $295 \times 100 \mu\text{m}^2$ with the maximum illumination power on the MEMS scanner of $\sim 80 \text{ mW}$ ($\sim 27 \text{ mW}$ on the sample). A metalized coating on the mirror surface will help accommodate more power on the sample by help reflecting of the heat energy (less heat absorption). All images have 400×135 pixels with single-sided acquisition (only acquiring data during either forward or backward path of the driving signals).

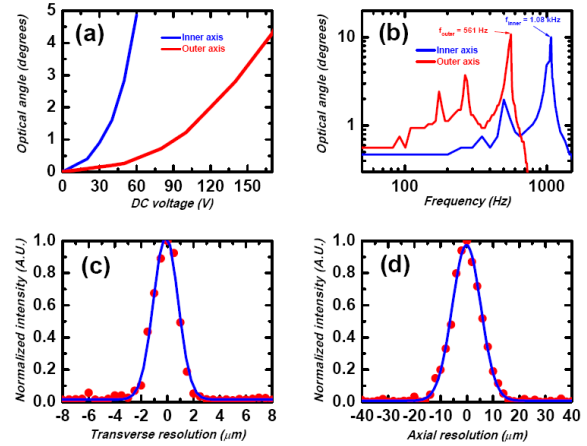


Fig. 2: Response characteristics of a $1 \text{ mm} \times 1 \text{ mm}$ MEMS scanner. For both panels a and b the voltage signal was applied to only one of the two opposing comb banks for each rotational axis. a, Optical deflection angle as a function of DC voltage. The maximum deflection angles are ± 5.0 degrees and ± 4.3 degrees for the inner (blue solid curve) and outer (red solid curve) axes, respectively. b, Frequency response functions for the inner (blue solid curve) and outer (red solid curve) axes. c and d, Determination of transverse (red dots) and axial (red dots) resolutions using normalized line images of single 100-nm-diameter fluorescent beads, respectively. Solid lines are Gaussian fits.

No post-image processing is performed on the images. The working distance in air is $280 \mu\text{m}$ from the GRIN objective tip. To characterize imaging resolution of the 2PFME, we visualized 100-nm-diameter fluorescent beads [Fig. 3(c) and Fig. 3(d)]. The transverse and axial resolutions are estimated by the FWHM of curve fits to bead images, are $1.6 \mu\text{m}$ and $13.5 \mu\text{m}$, respectively. These values are comparable to previously reported microendoscopy resolution measurement [10]. The minor degradation in resolution is from the light exiting the PBF slightly overfilling both the MEMS mirror and the back aperture of the objective lens.

To demonstrate *in vivo* imaging, we anesthetized adult mice with a ketamine-xylazine cocktail, performed a 2.5-mm diameter craniotomy (right above the neocortex area—coordinates: -2 mm lambda and -2.5 mm lateral)), and intravenously injected $200 \mu\text{L}$ of fluorescein isothiocyanate-dextran (FITC-DEXTRAN, Mw 10000) in saline solution (58.3 mg/mL) into the tail. The FITC-DEXTRAN brightly labels the blood plasma, allowing us to image blood vessels near the neocortical surface [Figure 3(a) to 3(c)]. Due to successive, rapid line scans (560 Hz) from the MEMS scanner, we observed a procession of dark objects moving across a

sea of fluorescently labeled blood plasma [Figure 3(d)]. The dark spots are the red blood cells (RBCs), which exclude the dye and therefore are not fluorescent. The change in position of the spots between successive linescan is proportional to the velocity. In this imaging mode, the data comprise of a matrix with one spatial (y) dimension in the vertical axis and one temporal (t) dimension in the horizontal axis. The motion of RBCs leads to dark bands or streaks in the data set. The slopes of these streaks (dy/dt) in the image spans (measuring from the centerline of the streaks) directly translate to the velocity of the RBCs (an inset in Figure 3(d)). In these examples, the average velocity of the RBCs in Figure 3(d) is 51.9 ± 12.3 . The data are comparable to previously reported measurement [4]. In summary, we have created a 2-D MEMS based portable 2PFME imaging device that achieves micron-scale resolution with weight less than 3 g. The 2PFME achieves a large FOV and a fast linescan rate enabling functional imaging in live subjects. Such a compact imaging instrument should be useful for a broad range of intravital imaging purposes.

REFERENCES

- [1] A. Villringer, U. Dirnagl, "Coupling of brain activity and cerebral blood flow: basis of functional neuroimaging," *Cereb. Brain Metab.*, vol. Rev. 7, pp. 240-276, 1995.
- [2] V. A. Dirnagl U., Einhaupl K.M., "In-vivo confocal scanning laser microscopy of the cerebral microcirculation," *J Microsc.*, vol. 165, pp. 147-157, 1992.
- [3] W. Denk, *et al.*, "Two-photon laser scanning fluorescence microscopy," *Science*, vol. 248, pp. 73-76, April 6, 1990 1990.
- [4] D. Kleinfeld, *et al.*, "Fluctuations and stimulus-induced changes in blood flow observed in individual capillaries in layers 2 through 4 of rat neocortex," *Proc Natl Acad Sci U S A*, vol. 95, pp. 15741-6, Dec 22 1998.
- [5] W. Piyawattanametha and T. D. Wang, "MEMS-Based Dual-Axes Confocal Microendoscopy," *Selected Topics in Quantum Electronics, IEEE Journal of*, vol. PP, pp. 1-11, 2009.
- [6] F. Helmchen, *et al.*, "A miniature head-mounted two-photon microscope. high-resolution brain imaging in freely moving animals," *Neuron*, vol. 31, pp. 903-12, Sep 27 2001.
- [7] C. J. Engelbrecht, *et al.*, "Ultra-compact fiberoptic two-photon microscope for functional fluorescence imaging in vivo," *Opt. Express*, vol. 16, pp. 5556-5564, 2008.
- [8] R. Weissleder and M. J. Pittet, "Imaging in the era of molecular oncology," *Nature*, vol. 452, pp. 580-589, 2008.
- [9] H. Bao, *et al.*, "Fast handheld two-photon fluorescence microendoscope with a $475 \mu\text{m} \times 475 \mu\text{m}$ field of view for in vivo imaging," *Opt. Lett.*, vol. 33, pp. 1333-1335, 2008.
- [10] B. A. Flusberg, *et al.*, "In vivo brain imaging using a portable 3.9 gram two-photon fluorescence microendoscope" *Opt Lett*, vol. 30, 2005.
- [11] W. Piyawattanametha, *et al.*, "Fast-scanning two-photon fluorescence imaging based on a microelectromechanical systems two-dimensional scanning mirror," *Optics Letters*, vol. 31, pp. 2018-2020, July 1, 2006.
- [12] W. Piyawattanametha, *et al.*, "A Portable Two-photon Fluorescence Microendoscope Based on a Two-dimensional Scanning Mirror," in *Optical MEMS and Nanophotonics, 2007 IEEE/LEOS International Conference on*, 2007, pp. 6-7.
- [13] W. Jung, *et al.*, "Miniaturized probe based on a microelectromechanical system mirror for multiphoton microscopy," *Opt. Lett.*, vol. 33, pp. 1324-1326, 2008.
- [14] T.-M. Liu, *et al.*, "Miniaturized multiphoton microscope with a 24Hz frame-rate," *Opt. Express*, vol. 16, pp. 10501-10506, 2008.
- [15] C. L. Hoy, *et al.*, "Miniaturized probe for femtosecond laser microsurgery and two-photon imaging," *Opt. Express*, vol. 16, pp. 9996-10005, 2008.
- [16] H. Ra, *et al.*, "Two-Dimensional MEMS Scanner for Dual-Axes Confocal Microscopy," *Microelectromechanical Systems, Journal of*, vol. 16, pp. 969-976, 2007.

CONTACT

*W. Piyawattanametha can be reached at wibool@gmail.com.